Journal of Biomechanics 87 (2019) 83–92

Contents lists available at ScienceDirect

Journal of Biomechanics

journal homepage: www.elsevier.com/locate/jbiomech
www.JBiomech.com

# Effect of simulated microgravity induced *PI3K-nos2b* signalling on zebrafish cardiovascular plexus network formation

Xiang Xie [a,b,1], Daoxi Lei [a,1], Qian Zhang [a], Yeqi Wang [a,*], Lin Wen [a], Zhiyi Ye [a], Ahmad Ud Din [a], Dongyu Jia [c], Antonio Apicella [d], Guixue Wang [a,*]

[a] Key Laboratory of Biorheological and Technology of Ministry of Education, State and Local Joint Engineering Laboratory for Vascular Implants, Bioengineering College of Chongqing University, Chongqing 400030, China
[b] The School of Basic Medical Sciences, Southwest Medical University, Luzhou, Sichuan Province 646000, China
[c] Department of Biology, Georgia Southern University, Statesboro, GA 30460, USA
[d] Advanced Materials Lab, Polytechnic and Base Science School of University of Campania, San Lorenzo, 81031, Italy

ARTICLE INFO

*Article history:*
Accepted 22 February 2019

*Keywords:*
CVP network formation
*Nos2b*
*PI3K*
Simulated microgravity
Zebrafish

ABSTRACT

Local abnormal angiogenesis and cardiovascular system reorganization have been observed in embryos exposed to a simulated microgravity (SM) environment. In this study, changes in key molecular signals and pathways in cardiovascular development have been investigated under microgravity conditions. In particular, the caudal vein plexus (CVP) network, formed by sprouting angiogenesis has been chosen. Zebrafish embryos were exposed to SM using a ground-based microgravity bioreactor for 24 and 36 h. The SM was observed to have no effect on the zebrafish length, tail width and incubation time whereas it was observed to significantly reduce the heart rate frequency and to promote abnormal development of the CVP network in the embryos. Nitric oxide (NO) content demonstrated that the total proteins in zebrafish embryos were significantly higher in SM than in the control group grown under normal conditions. It was then preliminarily determined how NO signals were involved in SM regulated zebrafish CVP network formation. *nos2b* MO was injected and CVP network evolution was observed in 36 h post fertilization (hpf) under SM condition. The results showed that the CVP network formation was considerably decreased in the *nos2b* MO treated group. However, this inhibition of the CVP network development was not observed in control MO group, indicating that *nos2b* is involved in the SM-regulated vascular development process in zebrafish. Moreover, specific phosphoinositide 3-kinase (*PI3K*) inhibitors such as LY294002 were also tested on zebrafish embryos under SM condition. This treatment significantly inhibited the formation of zebrafish CVP network. Furthermore, overexpression of *nos2b* partly rescued the LY294002-caused CVP network failure. Therefore, it can be concluded that SM affects zebrafish CVP network remodeling by enhancing angiogenesis. Additionally, the *PI3K-nos2b* signaling pathway is involved in this process.



## 1. Introduction

Exposure to microgravity during space expeditions has been shown to induce many changes to the physiological systems of astronauts. These changes include loss of bone mineral density, muscle atrophy, cardiovascular deconditioning, and impairment of pulmonary function (Crawford-Young, 2006). Specifically, the cardiovascular system is particularly affected during space flight, with changes manifesting themselves as cardiac dysrhythmias and atrophy, orthostatic intolerance, and reduced aerobic capacity (Convertino, 2009). Further investigations into understanding the influence of the microgravity environment on the cardiovascular systems need to be conducted, in particular, its influence on blood vessel angiogenesis modifications needs to be better understood.

Angiogenesis is the process of new blood vessel formation from pre-existing endothelial structures (Folkman, 1995). Different behaviors have been observed in endothelial cells (ECs) cultured in modeled microgravity. The expression of many angiogenic molecules, such as nitric oxide (NO), vascular endothelial cell growth factor (VEGF), and endothelin-1 is modified under

* Corresponding authors.
*E-mail address:* wanggx@cqu.edu.cn (G. Wang).
[1] Contributed equally.

https://doi.org/10.1016/j.jbiomech.2019.02.019
0021-9290/

microgravity conditions, and therefore imply that microgravity influences the angiogenesis process (Griffoni et al., 2011; Infanger et al., 2007; Mariotti and Maier, 2008).

NO is synthesized in the vascular system by endothelial nitric oxide synthesis (*eNOS*) and is involved in maintaining blood vessels and their normal physiological functions (Huang et al., 2006). *eNOS* has been reported to affect the regulation of vascular tone, as well as vascular remodeling and angiogenesis (Huang et al., 1995; Kubes et al., 1991; Moncada et al., 1991; Murohara et al., 1998; Rudic et al., 1998). NO not only influences the early development of the cardiovascular system but also plays an important role in the angiogenesis process (Pelster et al., 2005). At present, homologues of *eNOS* have not identified in zebrafish but some studies have shown that the *nos2b* gene in zebrafish contains *eNOS*-specific functional domains, in particular the N-terminal myristoylation sequence (Lepiller et al., 2009). Based on these studies it can be hypothesized that *nos2b* in zebrafish could have the same function of *eNOS* in mammals. Therefore, it is necessary to better understand whether *nos2b* participates in the regulating of the zebrafish vascular development.

Increasing evidence has shown that NO is involved in simulated microgravity-induced angiogenesis. It has been reported that *in vitro eNOS* inhibitors block EC migration, proliferation, and tube formation under simulated microgravity conditions (Siamwala et al., 2010). Additionally, many growth factors and hormones have been shown to induce phosphoinositide 3-kinase-Akt (PI3K-Akt)-dependent phosphorylation of *eNOS*, which activates *eNOS* and induces subsequent increases in NO production (Goetze et al., 2002; Uruno et al., 2004). Also, it has been demonstrated that shear stress activates *eNOS* phosphorylation through the *PI3K-Akt* pathway (Dimmeler et al., 1999; Fisslthaler et al., 2000). However, little is known whether *PI3K-nos2b* signaling is involved in SM-induced zebrafish caudal vascular angiogenesis.

This study aimed to explore the effects of microgravity on zebrafish angiogenesis and related mechanisms. To investigate this process, we focused on the caudal vein plexus (CVP) network that is formed by sprouting angiogenesis. In particular, we attempted to clarify how simulated microgravity could affect vascular network angiogenesis during CVP development. The simulated microgravity-sensitive *PI3K-nos2b* signaling pathway has been hypothesized to be involved in controlling network formation of CVP. This study has been designed to analyze the mechano-transduction link between microgravity and angiogenesis, and to explain how microgravity regulates CVP network angiogenesis. In the near future, this study could provide new targets for rapid angiogenic therapy for microgravity-induced cardiovascular diseases and injuries.

## 2. Methods

### 2.1. Zebrafish (Danio rerio)

The animal housing and surgical procedures were carried out in accordance with the Guide for the Chinese Animal Care and Use Committee Standards, which conforms to the Guide for the Care and Use of Laboratory Animals published by the U.S. National Institutes of Health (NIH Publication No. 85-23, revised 1996). All animal handling procedures were also performed in accordance with protocols approved by the Animal Ethics Committee of Chongqing University (CHN). NIH guidelines for the care and use of laboratory animals (NIH Publication #85-23 Rev. 1985) were also observed.

This study used zebrafish *Tg (Flk1:GFP)* that express the green fluorescent protein in their endothelial cells. The zebrafishes were obtained from Tsinghua University (CHN) developmental biology lab and then bred and maintained in the laboratory at Chongqing University.

### 2.2. Zebrafish embryos exposition to SM

An MG-IIA type ground-based rotating bioreactor was provided by the Institute of Mechanics at Chinese Academy of Sciences (CHN) has been utilized to SM. Zebrafish embryos from the same mother were divided into two equivalent groups: the SM group and the control group. Zebrafish embryos for the SM experiments were first placed in embryo culture containers and then successively tested in the rotating bioreactor (Fig. 1A), while the control group embryos were placed in the same type of embryo culture containers but tested in a stationary state. The culture container radius was 2.5 cm, and 60 fertilized embryos were placed in each container for each experimental group. Air bubbles were removed, and the container was sealed and mounted on the bioreactor base. All embryos were placed on the same table and received the same vibration and illumination time. We monitored zebrafish length and tail width, zebrafish incubation, heart rate, and development of CVP at 24 h post fertilization (hpf) and 36 hpf. In previous experiments the horizontal rotary cultivation was found to (the treatment time was from 24 hpf–36 hpf) promote apoptosis of zebrafish cells and had no significant effect on proliferation, and therefore resulted in a delayed development of embryo tail's vascular plexus during angiogenesis at 36 hpf (Sun et al., 2013). In this study, we wanted to explore the effect of microgravity on the early vascular development process in zebrafish. The somite stage for a zebrafish begins at 10–12 hpf, which is also the period in which embryonic cell morphogenesis and somite formation begins (Kimmel et al., 1995). Therefore, all tests were performed from 12 hpf in this study.

The MG-IIA ground-based bioreactor is made up of four parts including a rotating stent, tissue culture containers, a base stand, as well as a motor and transmission system (Fig. 1). There is no changing medium in this bioreactor. The bioreactor has a gas exchange membrane on both sides that provides oxygen for the bioreactor. In the rotating bioreactor, zebrafish embryos experience gravity, buoyancy, and centripetal forces, and are also subject to shear stresses. The trajectories of embryos are dependent on their dimensions, relative density, rotating speed, as well as other factors (Liu et al., 2004). If the solution has the same density as the embryos, there is no relative displacement when the acting forces on the embryos offset each other. This is similar to what happens in space microgravity and the MG-IIA type of ground-based bioreactor simulates it. The radius of the container can range from $0\ \text{cm} \le r \le 2.5\ \text{cm}$, while the rotation speed can be set at $5\ \text{rpm} \le n \le 50\ \text{rpm}$, then if $g_0$ 981 cm/s$^2$ is taken as gravity acceleration the angular velocity is:

$$\omega = \frac{n \times 2\pi}{60},$$

and the characteristic parameter for describing microgravity environment (K), can be then evaluated for our zebrafish embryos as seen below

$$K = \frac{\omega^2 r}{g_0}$$

According to zebrafish embryos dimensions and experimentally available testing conditions, critical values of K kept at the order of $10^{-2}$ (from $0.07 \times 10^{-2}$ at 5 rpm to $6.98 \times 10^{-2}$ at 50 rpm) suggests that the zebrafish embryos in the containers could be considered to undergo microgravity in all the testing conditions allowed by the bioreactor. However, embryos have to be kept in a state of suspension that avoids larger shear forces and bubble generation. Three-dimensional culture systems should create a moderate mechanical

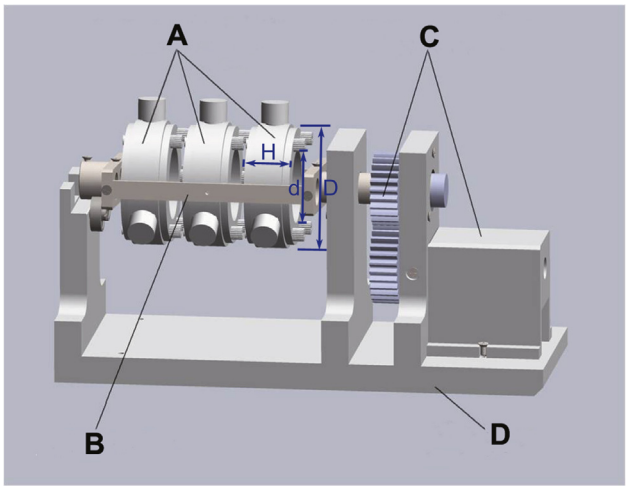


**Fig. 1.** The MG-IIA type of ground-based simulated microgravity (SM) bioreactor. The SM bioreactor was provided by the National Microgravity Laboratory, Institute of Mechanics, Chinese Academy of Sciences. (A) Tissue culture container. The inside diameter "d" is 5 cm, the outside diameter "D" is 8.5 cm, the high "H" is 3 cm. (B) Rotating stent. (C) Motor and Transmission system. (D) Base stand.

environment for the incubation of embryos. Some studies have shown that rotating speeds that are limited between 8.5 rpm and 26.5 rpm lead to preferable microgravity conditions (Lindsey et al., 2011). However, among these preferable limits, the commonly adopted rotating speeds for microgravity simulation experiments range from 15 rpm to 20 rpm (Moorman et al., 2002). In this study, due to diameter of the tested zebrafish embryos diameter being approximately 1 mm, which is larger than conventional embryos, a rotating speed near to the upper limit of 25 rpm was chosen to satisfy both the mechanical and dissolved oxygen concentration requirements (Kwon et al., 2008).

### 2.3. Treatment of zebrafish with a P13K signaling inhibitor

In order to clarify if the effect of SM on zebrafish CVP network formation is mediated by *PI3K* signaling, *flk1*: GFP embryos were treated with *PI3K* specific inhibitor LY294002 (Sigma-Aldrich, USA), 25 μM, dimethyl sulfoxide [DMSO] carrier content was 0.1%, n = 60) and control (DMSO)(0.1% DMSO, n = 60) under SM condition.

### 2.4. Morpholinos and micro-injections

Anti-sense morpholino oligonucleotides (MOs, Gene Tools LLC, USA) targeted to interfere with *nos2b* (MO; 5′GACCTGGTTGCCCATGTGTTTCTGA 3′), was designed over intron-exon junctions 1, 11 and 12, respectively. A mismatch (scramble) MO (scr; 5′ ACTCTGTCAACGGACACAAGACACT 3′) with no sequence homology to the zebrafish genome was used as a control. MOs were dissolved in sterile water to a final concentration of 500 μM. Fertilized eggs were then injected with approximately 3–4 ng of either MO at the 1–2 cell stage. For the "rescue" study, *nos2b* mRNA (100 ng/μl) was co-injected with the LY204002. Injected embryos and non-injected embryos were placed in a 28 °C incubator until 36 hpf for further use.

### 2.5. Reverse transcription (RT)-quantitative PCR (q-PCR)

Total RNA was extracted from zebrafish derived from both the treatment group and control group using a TianGen Kit according to the manufacturer's instructions. The total RNA concentration was determined by optical density using a spectrophotometer. After removing residual DNA with DNase I, equal amounts of RNA (1 mg) were added to a reverse transcriptase reaction mixture with oligo-dT primers (Invitrogen, USA). The power SYBR Green RT-PCR Kit (Applied Biosystems, Foster City, CA) was used to perform quantitative RT-PCR on a Bio-Rad CFX96 Real-Time system (Bio-Rad Laboratories, Inc., Hercules, CA). The expression level was analyzed and normalized to β-actin in the cDNA samples. The primers used were:

*flk1* (reverse primers: 5′-CCCTCCAGCAGAACTGACTCCTTAC-3′; forward primers: 5′-GAGAACGGAACCAACAAGATCCACGAG-3′),

*β-action* (reverse primers: 5′-CTCCATATCATCCCAGTTGGTGACA-3′; forward primers: 5′-CTGTCTTCCCATCCATCGTGGGTC-3′).

The quantitative PCR program was as follows: initial denaturation for 4 min at 94 °C, followed by 24 cycles of 94 °C for 1 min, 60 °C for 1 min and 72 °C for 1 min, and a final extension at 72 °C for 10 min. All the experiments were repeated 3 times in triplicate. The data was analyzed using the $^{\triangle\triangle}$Ct method. Independent experiments were performed three times, with three duplications in each independent experiment. The fold change to the gene expression was calculated using the statistical analysis method.

### 2.6. In situ hybridization

#### 2.6.1. Zebrafish embryo storage

Zebrafish embryos were fixed overnight at 4 °C in 4% paraformaldehyde then progressively dehydrated with methanol and stored in 100% methanol at −20 °C.

#### 2.6.2. The production of the probe

Specific primer sequences of *flk1* (910 bp) for in situ hybridization were designed. The PCR-fragments of zebrafish *flk1* cDNA were sub-cloned into a PMD-20T vector (TaKaRa, Japan). PCR with *flk1* (reverse primers: 5′-GATGCTATCCGACTGAACC-3′; forward primers: 5′-TGCCCAGATTATGGTGATG-3′) was performed on the recombinant plasmids. These PCR products were used as the template to synthesize digoxigenin (DIG)-labeled rib-probes using SP6 RNA polymerases (Roche, CH). The probes were purified after synthesis using mini Quick Spin RNA columns (Roche, CH). Sequence identification was performed by Invitrogen.

#### 2.6.3. Whole-mount in situ hybridizations

In our experiments, zebrafish was separately treated from 12 hpf to either 24 hpf or 36 hpf. The shell of the zebrafish embryo was stripped, and embryos were collected with EP tubes. Whole-mount in situ hybridization (WISH) experiments were performed as described (see: http://zfin.org/zf_info/zfbook/chapt9/9.8.html) on embryos fixed at 24 hpf and 36 hpf. Embryos were cleared in graduated concentrations of glycerol up to 80% before observations. At least 30 embryos were examined and demonstrated similar expression patterns. A minimum of three independent experiments was conducted per analysis. Lateral and dorsal views were imaged by a dissecting microscope (SZX9 Olympus).

### 2.7. Protein extraction and NO detection

In order to extract proteins, embryos were first washed three times with ice-cold phosphate-buffered saline and then disintegrated by grinding with cell-lysis solution containing 1% phenyl methane sulfonyl fluoride and protease inhibitors. The mixture was collected in micro-centrifuge tubes pre-chilled to 4 °C and centrifuged at 10000 rpm for 5–10 min and the supernatant was collected. The presence and concentration of NO was determined using a NO kit (JC bio, Nanjing, China) according to the manufacturer's instructions. NO content was obtained by fitting the data to the following function:

$$N = (Adet - Ablk)/(Astd - Ablk) \times B \div C$$

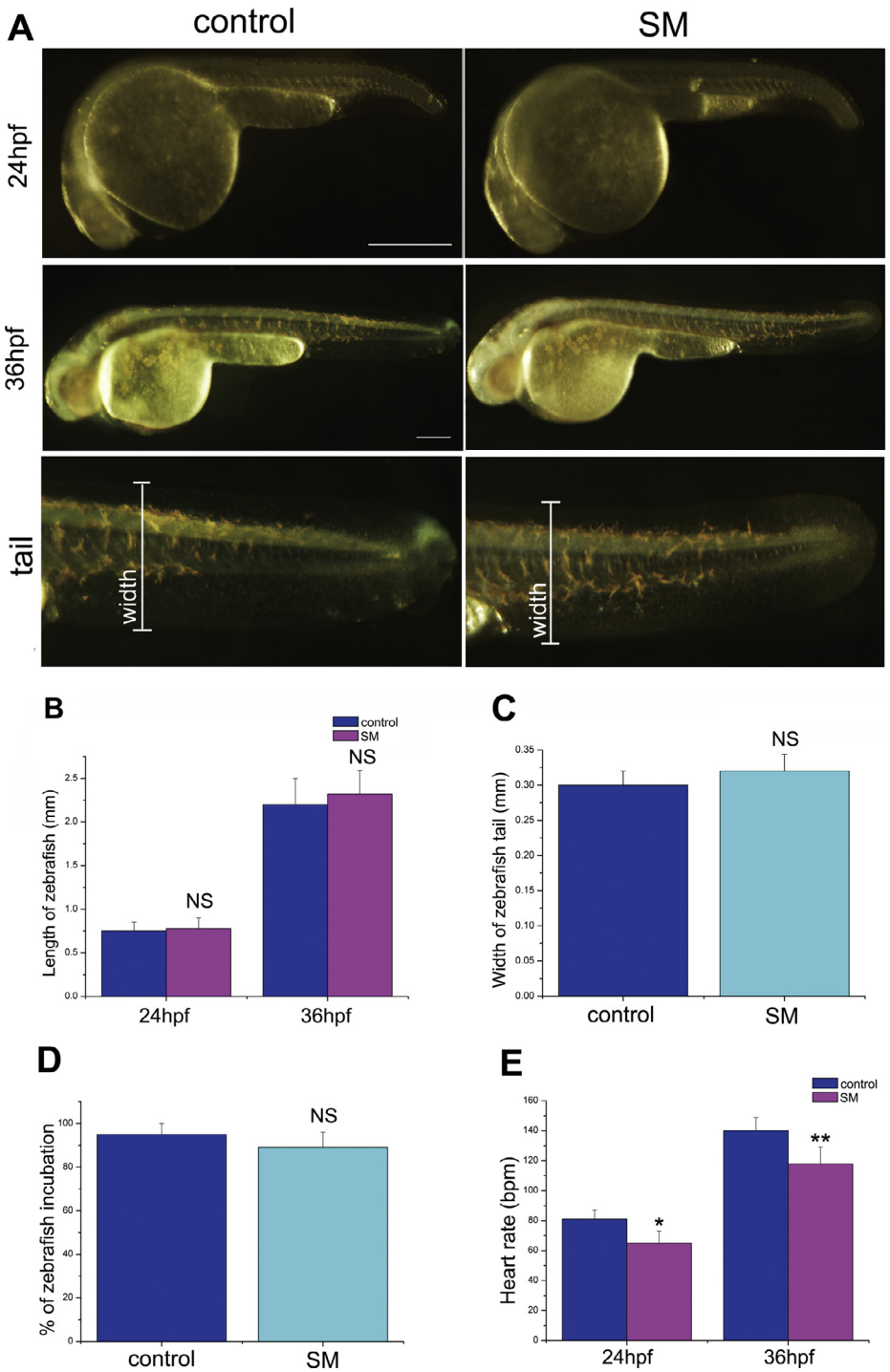


**Fig. 2.** SM affected zebrafish heart rate. (A) Brightfield images of SM treatment embryos at 24 hpf and 36 hpf. Scale bar, 200 μm. (B) The length of embryos (n = 60) at 24 hpf and 36 hpf after treated with SM from 12 hpf. (mean ± SD, *t* test). (C) The width of zebrafish embryos (n = 60) at 36 hpf. (mean ± SD, *t* test). (D) The zebrafish incubation (n = 60) was normal in SM group at 36 hpf. (mean ± SD, *t* test). (E) Heart rate of embryos (n = 60) as manual statistic counted at 24 hpf and 36 hpf. (mean ± SD, *t*-test, *P < 0.05, **P < 0.01).

where N is NO content (μmol/gprot), Adet is determined, Ablk is blank, Astd is the standard OD value, B is the standard sample concentration (20 μmol/L), and C is the sample protein concentration under test.

### 2.8. Fluorescent microscopy

The vascular development was observed at 24 hpf and 36 hpf by fluorescent microscopy after that zebrafish embryos were anesthetized, by a short exposure to 0.02% tricaine, and fixed with 1.5% low melting agarose (Sigma-Aldrich, LLC., St. Louis, USA). After the observation, the embryos were awakened using fresh water and released into the fish tank.

### 2.9. Statistical analysis

The data obtained in this study were reported as means ± standard deviation. All experiments were representative of 3

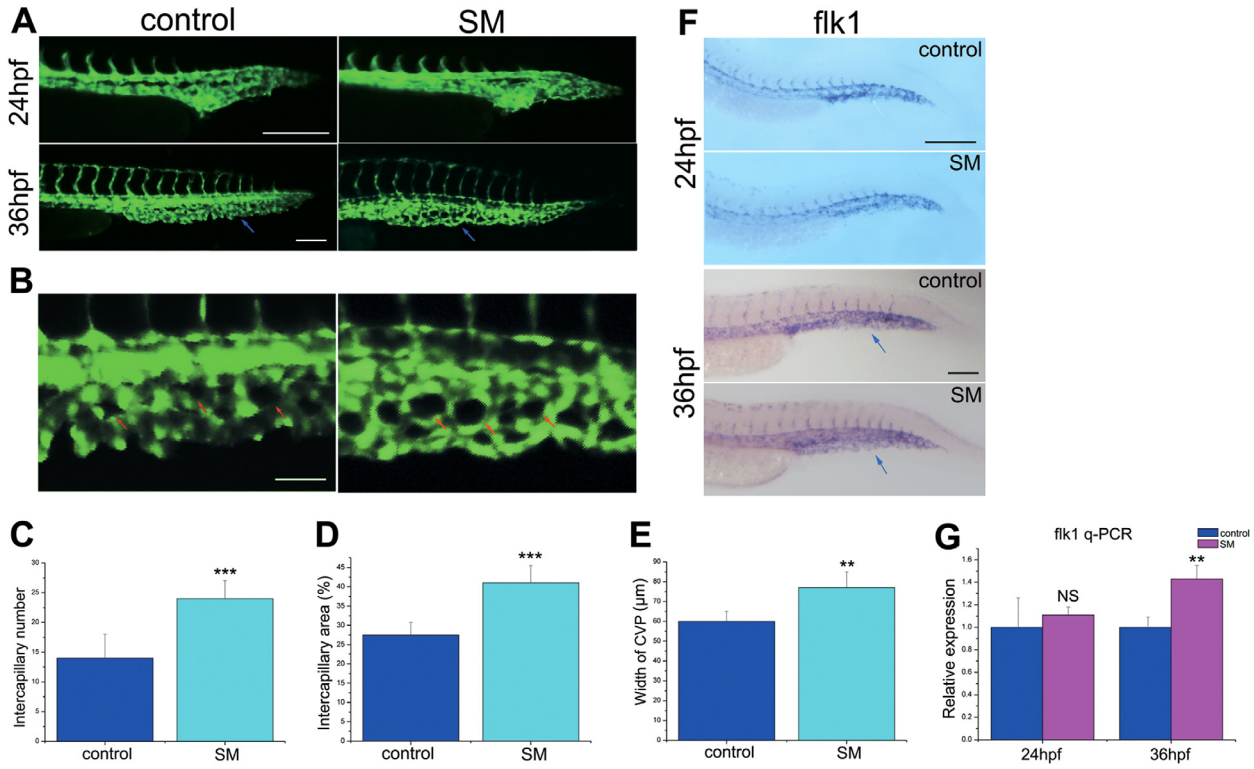


**Fig. 3.** SM regulated zebrafish CVP network formation. (A) Transgenic *flk1*: GFP embryos were treated with SM from 12 hpf and imaged by in vivo fluorescence microscopy at 24 hpf and 36 hpf. Representative examples from after SM treatment were shown. Lateral view, anterior to the left, dorsal is up. The CVP was indicated by blue arrows. Scale bar, 100 μm. (B) Higher magnification of the CVP region form (A). The intercapillary was indicated by red arrows. Scale bar, 50 μm. (C) The intercapillary number was counted. Total of thirty embryos were used for the counting in each case. (mean ± SD, *t*-test, ***P < 0.001). (D) The percentage of intercapillary area was quantified. Total of thirty embryos were used for the quantification in each case. (mean ± SD, *t*-test, ***P < 0.001). (E) The width of CVP was measured. Total of thirty embryos were used for the measurement in each case. (mean ± SD, *t*-test, **P < 0.01). (F) The *flk1* expression in developing CVP was increased by treating with SM. Scale bar, 100 μm. (G) qPCR results of zebrafish flk1 relative expression at 24 hpf and 36 hpf. (mean ± SD, *t*-test, **P < 0.01). (For interpretation of the references to colour in this figure legend, the reader is referred to the web version of this article.)

independent experiments. Data obtained from different treatment groups were statistically compared using SPSS v17.0. Statistical differences between experimental groups were evaluated using one-way ANOVA or Student's *t*-test. A single asterisk * in the legend denotes a significance level set at $P \leq 0.05$, a double asterisk ** refers to a $P \leq 0.01$, and a triple asterisk *** refers to a $P \leq 0.001$.

## 3. Results

### 3.1. SM regulates zebrafish CVP network formation

Venous tip cells in the caudal vein of zebrafish embryos sprout out at 24 hpf, and then they form a clear network with spaces between capillaries and fused Vasa Vasorum (VV) at 36 hpf. Embryos were treated in SM in order to determine whether it has an effect on the zebrafish CVP network formation. Zebrafish were treated with SM and it was observed that there was no effect on the zebrafish length, tail width and incubation (n = 60) (Fig. 2A–D), SM reduced the embryos heart rate (Fig. 2E). Previous studies have shown that reduced heart rate significantly affects angiogenesis (Branum et al., 2013; Brown et al., 2005). These results suggest that SM could have a significant effect on the cardiovascular system of zebrafish.

To verify this hypothesis, we analyzed the zebrafish CVP network development using a stereo microscope. As shown in Fig. 3A, embryo caudal vessels developed normally in the control and SM-treated groups at 24 hpf, suggesting that the caudal vascular development was normal before circulation. At 36 hpf, the CVP in the control group displayed a clear network, with spaces between capillaries and fused VV (Fig. 3A, B). However, the width of the CVP, the inter-capillary number of CVP, and the inter-capillary area of the CVP were significantly increased in the SM-treated group (Fig. 3A–E). Additionally, the expression of the vascular endothelial cell marker, *flk1*, in the CVP region by WISH and qPCR was investigated. At 24 h, *flk1* expression was normal in SM-treated embryos (Fig. 3F, G). However, *flk1* expression within the CVP and surrounding region was markedly increased in the SM-treated group at 36 hpf (Fig. 3F, G). These findings suggested that SM is a crucial moderator during CVP network formation in zebrafish.

### 3.2. nos2b is involved in SM-mediated CVP network formation

NO can regulate early cardiovascular development of zebrafish embryos and it plays an important role in supporting the vascular system during individual development. In order to know whether SM involved NO signaling in the development of zebrafish vascular processes, the NO concentration in zebrafish was verified. At 36 hpf, the NO concentration of the SM-treated group was higher than the that of the control group (Fig. 4B). This suggests that NO signaling may participate in the SM-regulated vascular development process in zebrafish.

The *nos2b* gene in zebrafish may play a role in the process of angiogenesis similar to *eNOS* in mammalian cells. In order to evaluate whether *nos2b* participates in CVP network development induced by SM, we injected *nos2b* MO into zebrafish embryos at the 1–4 cell period and then treated them with SM until 36 hpf. It was found that the width of the CVP, the inter-capillary number of CVP and the inter-capillary area of the CVP were significantly

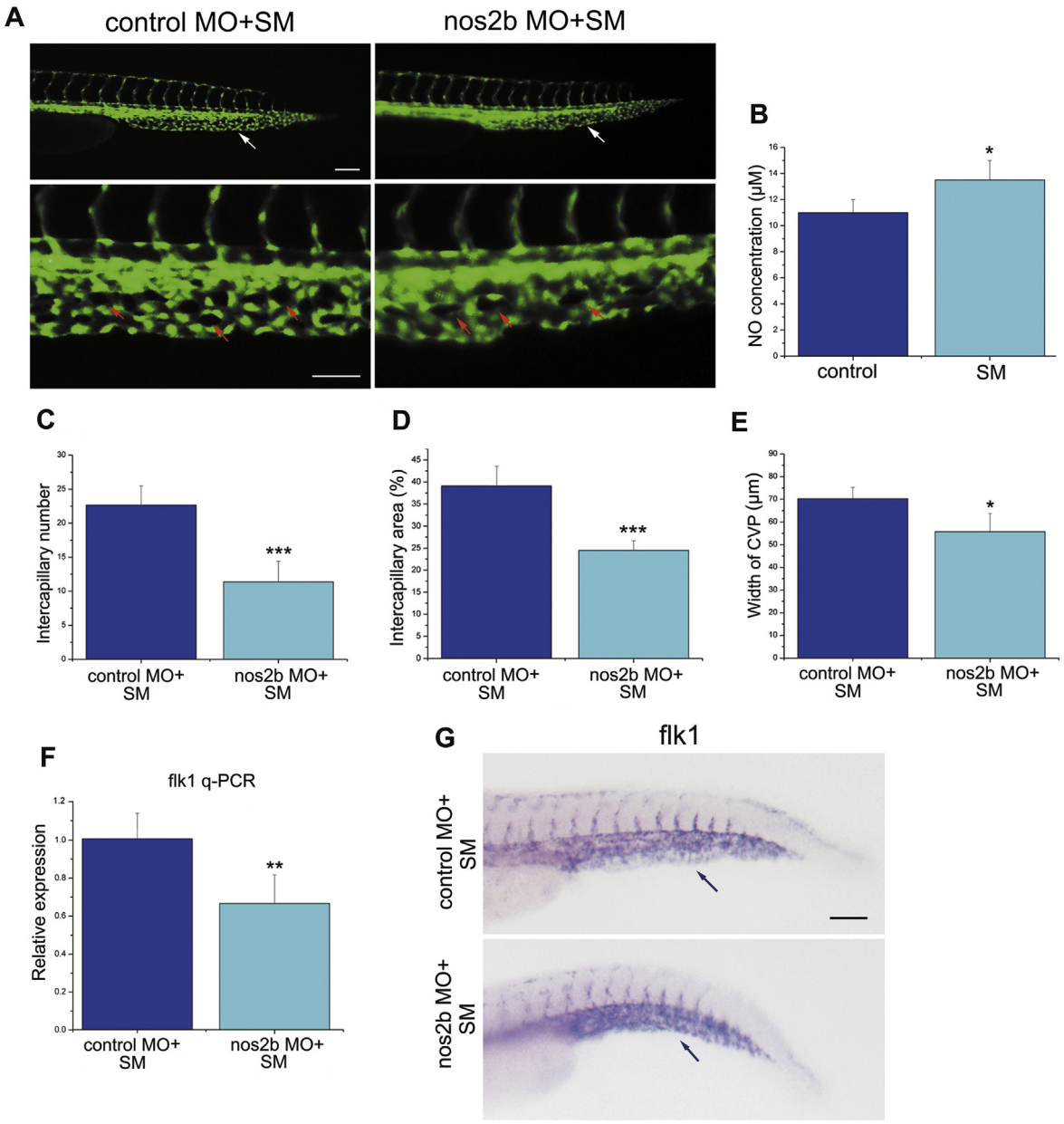


**Fig. 4.** nos2b was a pivotal factor in SM-regulating CVP network formation. (A) The fluorescence microscopy images of embryos at 36 hpf. Lateral view, anterior to the left, dorsal is up. The CVP was indicated by white arrows. Scale bar, 100 μm. Under panel showed higher magnification of the CVP region form above picture. The intercapillary was indicated by red arrows. Scale bar, 50 μm. (B) The NO concentration of zebrafish under SM and control conditions at 36 hpf. (mean ± SD, *t*-test, *P < 0.05). (C) The intercapillary number was counted. Total of thirty embryos were used for the counting in each case. (mean ± SD, *t*-test, ***P < 0.001). (D) The percentage of intercapillary area was quantified. Total of thirty embryos were used for the quantification in each case. (mean ± SD, *t*-test, ***P < 0.001). (E) The width of CVP was measured. Total of thirty embryos were used for the measurement in each case. (mean ± SD, *t*-test, *P < 0.05). (F) qPCR results of zebrafish flk1 relative expression at 36 hpf. (mean ± SD, *t*-test, **P < 0.01). (G) The *flk1* expression injected nos2b MO was decreased under SM condition. Scale bar, 100 μm. (For interpretation of the references to colour in this figure legend, the reader is referred to the web version of this article.)

decreased in the *nos2b* MO + SM-treated group compared with the control MO + SM group (Fig. 4A, C–E). It was also found that the size of the *flk1* expression domain in the CVP region was reduced in *nos2b* MO-injected embryos (Fig. 4F, G). These findings suggest that *nos2b* is a possible downstream factor of SM in zebrafish CVP network formation.

### 3.3. SM-induced PI3K signaling is necessary for zebrafish CVP network formation

Many studies have shown that *PI3K* signaling is the central pathway induced by SM (Dai et al., 2014; Kang et al., 2011; Shi et al., 2012). In order to evaluate possible mechanisms of enhanced CVP network development induced by SM, a *PI3K* signaling inhibitor was used as a co-treatment with SM and then the effect was analyzed using fluorescence imaging, qPCR and in situ hybridization. As seen in Fig. 5A co-treatment with SM and LY294002 partially recovered the SM-induced CVP capillary network increase. Additionally, the width of the CVP, the intercapillary number of CVP, and the intercapillary area of the CVP were significantly decreased in LY294002 + SM group (Fig. 5B–D). Meanwhile, the expression of *flk1* in the CVP area in the LY294002 + SM treated group was significantly decreased when compared with the SM group at 36 hpf (Fig. 5E, F). These results demonstrate that the

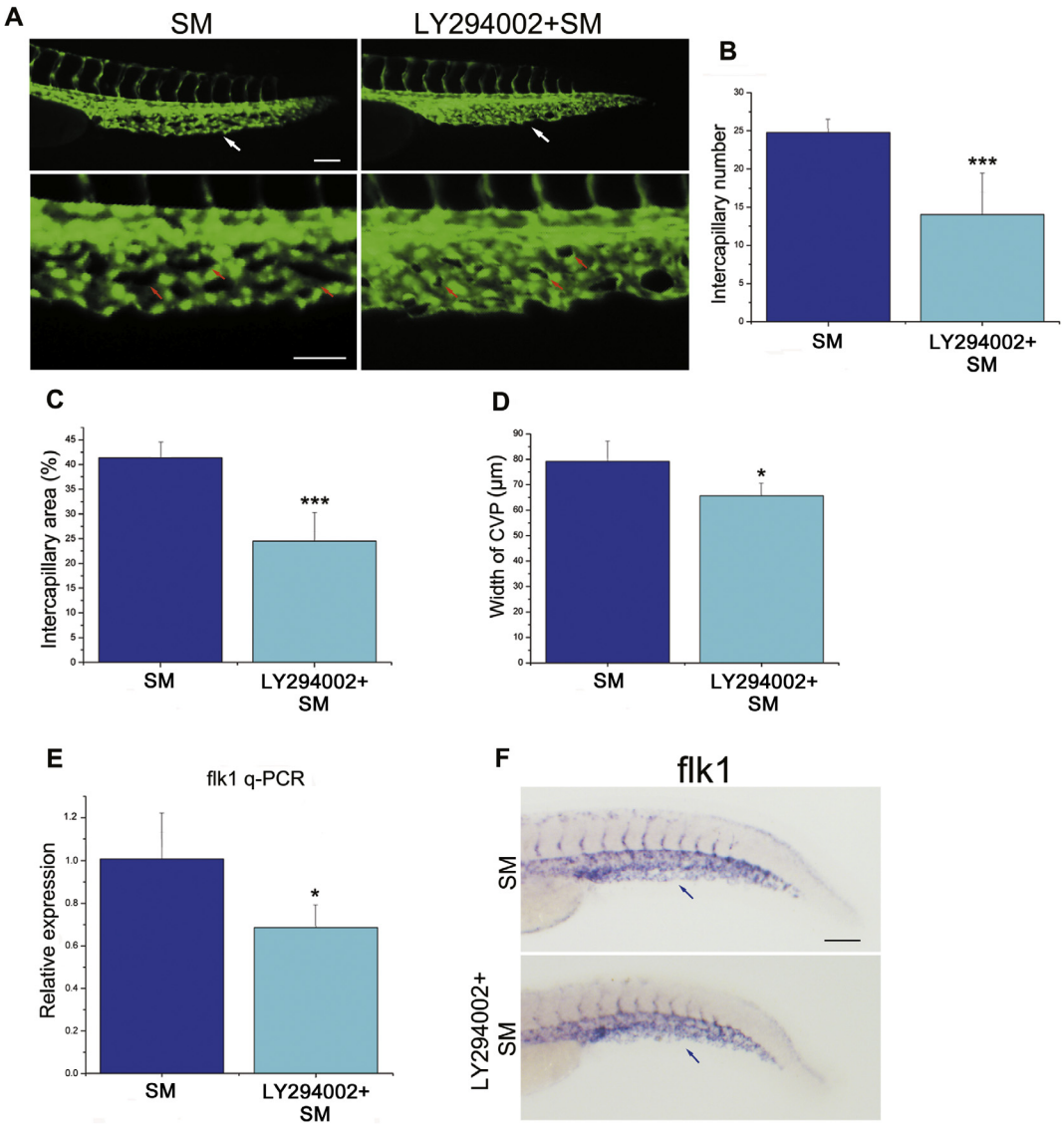


**Fig. 5.** SM regulated CVP network formation via PI3K signaling. (A) LY294002 contribution to CVP network formation was assessed by fluorescence microscopy at 36 hpf. Lateral view, anterior to the left, dorsal is up. The CVP was indicated by white arrows. Scale bar, 100 μm. Under panel showed higher magnification of the CVP region form above picture. The intercapillary was indicated by red arrows. Scale bar, 50 μm. (B) The intercapillary number was sharply reduced in LY294002 + SM group. (n = 30) (mean ± SD, *t*-test, ***P < 0.001). (C) The percentage of intercapillary area was quantified. (n = 30) (mean ± SD, *t*-test, ***P < 0.001). (D) The width of CVP was measured. Total of thirty embryos were used for the measurement in each case. (mean ± SD, *t*-test, *P < 0.05). (E) qPCR results of zebrafish flk1 relative expression at 36 hpf. (mean ± SD, *t*-test, *P < 0.05). (F) Whole In situ hybridization for *flk1* in caudal area at 36 hpf. Scale bar, 100 μm. (For interpretation of the references to colour in this figure legend, the reader is referred to the web version of this article.)

SM-induced CVP network development is achieved via *PI3K* signaling.

### 3.4. The PI3K-nos2b signaling cascade plays a role in SM regulated zebrafish CVP network formation

Activation of the survival signal *PI3K/Akt* and the endothelial specific *eNOS*/NO pathway is closely associated with vascular angiogenesis and remodeling (Dayanir et al., 2001; Lee et al., 2006). In this study it was that the NO concentration significantly decreased with the addition of LY294002 (Fig. 6A). Therefore, it was assumed that *PI3K* signaling could regulate *nos2b* activity to mediate CVP network formation. To confirm this, zebrafish embryos were first injected with *nos2b* mRNA at the 1–4 cell period and then treated with LY294002 from 12 hpf to 36 hpf. As shown in Fig. 6D, the CVP was inhibited, in the LY294002-treated group, failing to make proper connections with neighboring sprouts. However, CVP in the LY294002 + *nos2b* mRNA group did not exhibit these apparent vascular abnormalities. The width of the CVP, the CVP inter-capillary number, and the area were partly recovered by *nos2b* mRNA treatment (Fig. 6B, C, E). In addition, the expression of *flk1* remained low in the LY294002 group, while the level of *flk1* recovered in the LY294002 + *nos2b* mRNA group was similar to the control group (Fig. 6F). The data shown here indicates that *nos2b* mRNA treatment partly rescues the LY294002-induced CVP network formation failure. Whole-mount in situ hybridization also showed the same result (Fig. 6G). These results suggest that SM acts via *PI3K-nos2b* signaling to regulate CVP network formation.

## 4. Discussion

During manned space flights, the human body is exposed to microgravity, and several cardiovascular dysfunction phenomena

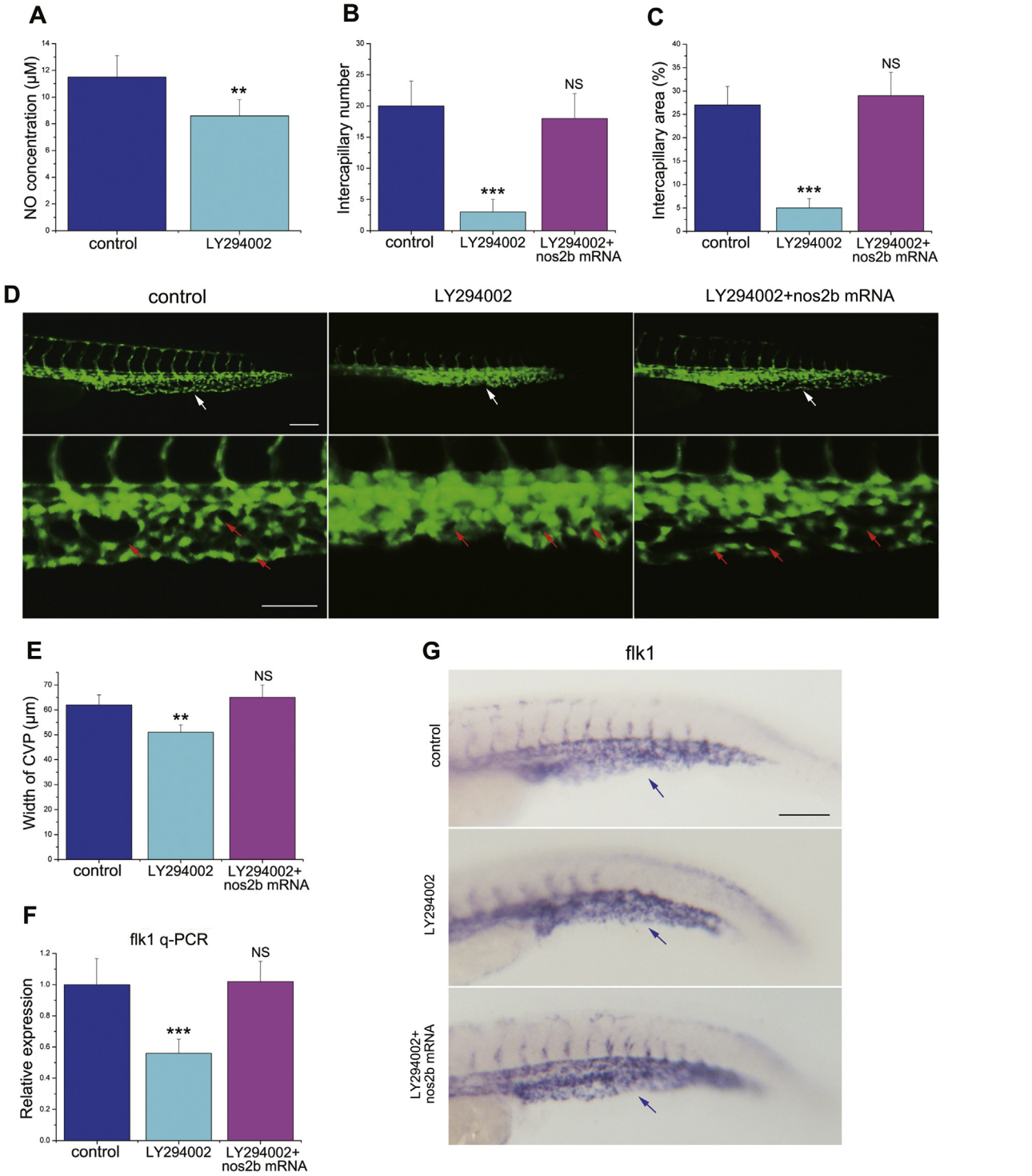


**Fig. 6.** SM-mediated PI3K regulated nos2b during CVP network formation in zebrafish. (A) The NO concentration of zebrafish was detected at 36 hpf. (mean ± SD, *t*-test, **P < 0.01). (B) *nos2b* mRNA segmental rescued the intercapillary number in LY294002 treated embryos. (n = 30)(mean ± SD, *t*-test, ***P < 0.001). (C) The percentage of intercapillary area also could be partly rescued by *nos2b* mRNA. (n = 30)(mean ± SD, ANOVA, ***P < 0.001). (D) The fluorescence microscopy images of embryos at 36 hpf. Lateral view, anterior to the left, dorsal is up. The CVP was indicated by white arrows. Scale bar, 100 μm. Under panel showed higher magnification of the CVP region form above picture. The intercapillary was indicated by red arrows. Scale bar, 50 μm. (E) The width of CVP could recover via *nos2b* mRNA. (n = 30)(mean ± SD, ANOVA, **P < 0.01). (F) qPCR results of zebrafish flk1 relative expression at 36 hpf. (mean ± SD, ANOVA, ***P < 0.001). (G) Whole In situ hybridization for *flk1* in caudal area at 36 hpf. Scale bar, 100 μm. (For interpretation of the references to colour in this figure legend, the reader is referred to the web version of this article.)

have been observed (Antonutto and di Prampero, 2003). Particularly, the mechanism of microgravity-regulated endothelial differentiation and vascular development is not yet clear. In this study, SM was found to affect the zebrafish CVP network formation. Additionally, the CVP network formation was found to be regulated in SM via the activation of the *PI3K-nos2b* signaling pathway. In this study a previously unrecognized role of SM in zebrafish angiogenesis was revealed and the underlying mechanisms as well as novel complementary explanations for microgravity-induced vascular remodeling were identified.

Angiogenesis, a process by which new blood vessels are formed, plays an important role in physiological and pathological processes

in humans. In the vascular development process of zebrafish, the main arterial and venous blood vessels, cardiac primordia, and the original embryonic capillary network are formed from 12 hpf to 36 hpf (Yancopoulos et al., 2000). A zebrafish heart starts to beat and blood starts to circulate in the body at 24 hpf. At the beginning of the establishment of blood circulation, primitive vascular plexus shows a great deal of plasticity during the process of vascular development. Large blood vessels became wide, some small blood vessels promptly disappear, and some fragments of the blood vessels begin to form new blood vessels (Buschmann et al., 2010; le Noble et al., 2004). However, effects of microgravity on zebrafish vascular angiogenesis are largely unknown. In this study, it was found that SM had no effect on the zebrafish vascular development at 24 hpf but promoted the CVP network formation from 24 to 36 hpf. Our previous studies indicated that blood flow plays an important role in CVP network formation(Xie et al., 2018). The results suggest that blood flow might contribute to CVP network formation during SM.

NO, which is locally produced in the endothelium, is an important mediator of blood flow, vascular permeability, and angiogenesis (Namkoong et al., 2008; Sessa, 2009). The *eNOS*-derived NO is a crucial contributor to the maintenance of cardiovascular homeostasis. The *eNOS*/NO pathway has been shown to exert a permissive role in angiogenesis in adult organisms (Dulak and Józkowicz, 2002; Namkoong et al., 2005). In addition, inhibition of endogenously produced NO or disruption of the *eNOS* gene has been found to reduce new blood vessel formation in animal models (Murohara et al., 1998; Ziche et al., 1997). Furthermore, both in vivo and *in vitro* studies have found that suppression of *eNOS* activation can inhibit angiogenesis (Chung et al., 2008). Microgravity is a mechanical factor and *nos2b* can be regarded as the *eNOS* homolog in zebrafish, and therefore based on the results of this study we suggest that *nos2b* may play an important role in SM-regulated CVP network formation. These results contribute greatly to advancing research on the effects of SM on vascular development.

It has been reported that *eNOS* is phosphorylated by the Akt protein kinase in ECs, and results in an increase of *eNOS* activity. *eNOS* activity plays a crucial role in the regulation of vascular tone, vascular remodeling, angiogenesis and NO production (Kureishi et al., 2000). Earlier studies have suggested that PI3K inhibitors attenuate the VEGF-induced increases to NO release in ECs and that VEGF stimulates Akt-mediated *eNOS* phosphorylation (Fulton et al., 1999). Moreover, NO has been shown to protect ECs from serum-deprivation-induced apoptosis and promote the formation of capillary-like structures on Matrigel in an Akt-dependent manner (Kureishi et al., 2000). Furthermore, it has been described that NO production in cultured ECs in response to shear stress is controlled by the Akt-dependent phosphorylation of *eNOS* (Dimmeler et al., 1999). Considering all these findings, it can be inferred that PI3K activates Akt, which in turn is responsible for regulating the phosphorylation and activation of *eNOS* (Igarashi et al., 2001). In this study we found that the *PI3K-nos2b* signaling cascade participated in SM-regulated CVP network formation in zebrafish. These results provide the first evidence that activation of *PI3K-nos2b* is a crucial event in SM-mediated signal transduction, favouring zebrafish angiogenesis.

## 5. Conclusions

This study suggests that SM plays a significant role in CVP network formation in zebrafish. SM influences CVP formation in zebrafish embryos by regulating *nos2b* expression via activated *PI3K* signaling. Notably, the signaling cascade that contains *PI3K* and *nos2b* may be a potential target for suppressing pathological angiogenesis. This offers important implications for cardiovascular disease therapy in the absence of gravity, such as what could occur during space flights.

## Acknowledgments

This study was partly supported by grants from the National Natural Science Foundation of China (11572064, 81400329), the National Key Technology R & D Program of China (2016YFC1102305, 2016YFC1101101) and the Fundamental Research Funds for the Central Universities (2018CDPTCG0001-10), the Special Support Program of Chongqing Postdoctoral Research Project (Xm2014027), Scientific Research Fund of SiChuan Provincial Education Department (17ZA0426, 17ZA0433), Luzhou City Bureau of Science and Technology (2016LZXNYD-J26) and the Visiting Scholar Foundation of Key Laboratory of Biorheological Science (CQKLBST-2016-004) as well as the supports from the Public Experiment Center of State Bioindustrial Base (Chongqing) and Chongqing Engineering Laboratory in Vascular Implants.

We are very grateful to Professor Anming Meng's laboratory at Tsinghua University, China for providing the zebrafish and to Professor Mian Long's laboratory at National Microgravity Laboratory, Institute of Mechanics, Chinese Academy of Sciences for partial experimental support. We also thank International Science Editing for editing this manuscript.

## Conflict of interest

The authors confirm that there is no financial or personal relationship with other people or organizations that could inappropriately influence (bias) this work.

## References

Antonutto, G., di Prampero, P.E., 2003. Cardiovascular deconditioning in microgravity: some possible countermeasures. Eur. J. Appl. Physiol. 90, 283–291.

Branum, S.R., Yamadafisher, M., Burggren, W.W., 2013. Reduced heart rate and cardiac output differentially affect angiogenesis, growth, and development in early chicken embryos (Gallus domesticus). Physiol. Biochem. Zool. 86, 370–382.

Brown, M.D., Davies, M., Hudlicka, O., 2005. Angiogenesis in ischaemic and hypertrophic hearts induced by long-term bradycardia. Angiogenesis 8, 253–262.

Buschmann, I., Pries, A., Styp-Rekowska, B., Hillmeister, P., Loufrani, L., Henrion, D., Shi, Y., Duelsner, A., Hoefer, I., Gatzke, N., Wang, H., Lehmann, K., Ulm, L., Ritter, Z., Hauff, P., Hlushchuk, R., Djonov, V., van Veen, T., le Noble, F., 2010. Pulsatile shear and Gja5 modulate arterial identity and remodeling events during flow-driven arteriogenesis. Development (Cambridge, England) 137, 2187–2196.

Chung, B.H., Kim, J.D., Kim, C.K., Kim, J.H., Won, M.H., Lee, H.S., Dong, M.S., Ha, K.S., Kwon, Y.G., Kim, Y.M., 2008. Icariin stimulates angiogenesis by activating the MEK/ERK- and PI3K/Akt/eNOS-dependent signal pathways in human endothelial cells. Biochem. Biophys. Res. Commun. 376, 404–408.

Convertino, V.A., 2009. Status of cardiovascular issues related to space flight: Implications for future research directions. Respir. Physiol. Neurobiol. 169 (Suppl 1), S34–37.

Crawford-Young, S.J., 2006. Effects of microgravity on cell cytoskeleton and embryogenesis. Int. J. Devel. Biol. 50, 183–191.

Dai, Z., Guo, F., Wu, F., Xu, H., Yang, C., Li, J., Liang, P., Zhang, H., Qu, L., Tan, Y., Wan, Y., Li, Y., 2014. Integrin alphavbeta3 mediates the synergetic regulation of core-binding factor alpha1 transcriptional activity by gravity and insulin-like growth factor-1 through phosphoinositide 3-kinase signaling. Bone 69, 126–132.

Dayanir, V., Meyer, R.D., Lashkari, K., Rahimi, N., 2001. Identification of tyrosine residues in vascular endothelial growth factor receptor-2/FLK-1 involved in activation of phosphatidylinositol 3-kinase and cell proliferation. J. Biol. Chem. 276, 17686–17692.

Dimmeler, S., Fleming, I., Fisslthaler, B., Hermann, C., Busse, R., Zeiher, A.M., 1999. Activation of nitric oxide synthase in endothelial cells by Akt-dependent phosphorylation. Nature 399, 601–605.

Dulak, J., Józkowicz, A., 2002. Nitric oxide and angiogenic activity of endothelial cells: direct or VEGF-dependent effect? Cardiovasc. Res. 56, 487–488.

Fisslthaler, B., Dimmeler, S., Hermann, C., Busse, R., Fleming, I., 2000. Phosphorylation and activation of the endothelial nitric oxide synthase by fluid shear stress. Acta physiologica Scandinavica 168, 81–88.

Folkman, J., 1995. Angiogenesis in cancer, vascular, rheumatoid and other disease. Nat. Med. 1, 27–31.
Fulton, D., Gratton, J.P., McCabe, T.J., Fontana, J., Fujio, Y., Walsh, K., Franke, T.F., Papapetropoulos, A., Sessa, W.C., 1999. Regulation of endothelium-derived nitric oxide production by the protein kinase Akt. Nature 399, 597–601.
Goetze, S., Bungenstock, A., Czupalla, C., Eilers, F., Stawowy, P., Kintscher, U., Spencer-Hansch, C., Graf, K., Nurnberg, B., Law, R.E., Fleck, E., Grafe, M., 2002. Leptin induces endothelial cell migration through Akt, which is inhibited by PPARgamma-ligands. Hypertension (Dallas, Tex. :1979) 40, 748–754.
Griffoni, C., Di Molfetta, S., Fantozzi, L., Zanetti, C., Pippia, P., Tomasi, V., Spisni, E., 2011. Modification of proteins secreted by endothelial cells during modeled low gravity exposure. J. Cell. Biochem. 112, 265–272.
Huang, P.L., Huang, Z., Mashimo, H., Bloch, K.D., Moskowitz, M.A., Bevan, J.A., Fishman, M.C., 1995. Hypertension in mice lacking the gene for endothelial nitric oxide synthase. Nature 377, 239–242.
Huang, S.-S., Wei, F.-C., Hung, L.-M., 2006. Ischemic Preconditioning Attenuates Postischemic Leukocyte - Endothelial Cell Interactions Role of Nitric Oxide and Protein Kinase C. Circ. J. 70, 1070–1075.
Igarashi, J., Bernier, S.G., Michel, T., 2001. Sphingosine 1-phosphate and activation of endothelial nitric-oxide synthase. differential regulation of Akt and MAP kinase pathways by EDG and bradykinin receptors in vascular endothelial cells. J. Biol. Chem. 276, 12420–12426.
Infanger, M., Ulbrich, C., Baatout, S., Wehland, M., Kreutz, R., Bauer, J., Grosse, J., Vadrucci, S., Cogoli, A., Derradji, H., Neefs, M., Küsters, S., Spain, M., Paul, M., Grimm, D., 2007. Modeled gravitational unloading induced downregulation of endothelin-1 in human endothelial cells. J. Cell. Biochem. 101, 1439–1455.
Kang, C.Y., Zou, L., Yuan, M., Wang, Y., Li, T.Z., Zhang, Y., Wang, J.F., Li, Y., Deng, X.W., Liu, C.T., 2011. Impact of simulated microgravity on microvascular endothelial cell apoptosis. Eur. J. Appl. Physiol. 111, 2131–2138.
Kimmel, C.B., Ballard, W.W., Kimmel, S.R., Ullmann, B., Schilling, T.F., 1995. Stages of embryonic development of the zebrafish. Dev. Dyn. 203, 253–310.
Kubes, P., Suzuki, M., Granger, D.N., 1991. Nitric oxide: an endogenous modulator of leukocyte adhesion. Proc. Natl. Acad. Sci. 88, 4651.
Kureishi, Y., Luo, Z., Shiojima, I., Bialik, A., Fulton, D., Lefer, D.J., Sessa, W.C., Walsh, K., 2000. The HMG-CoA reductase inhibitor simvastatin activates the protein kinase Akt and promotes angiogenesis in normocholesterolemic animals. Nat. Med. 6, 1004–1010.
Kwon, O., Devarakonda, S.B., Sankovic, J.M., Banerjee, R.K., 2008. Oxygen transport and consumption by suspended cells in microgravity: a multiphase analysis. Biotechnol. Bioeng. 99, 99–107.
le Noble, F., Moyon, D., Pardanaud, L., Yuan, L., Djonov, V., Matthijsen, R., Breant, C., Fleury, V., Eichmann, A., 2004. Flow regulates arterial-venous differentiation in the chick embryo yolk sac. Development (Cambridge, England) 131, 361–375.
Lee, S.J., Namkoong, S., Kim, Y.M., Kim, C.K., Lee, H., Ha, K.S., Chung, H.T., Kwon, Y.G., Kim, Y.M., 2006. Fractalkine stimulates angiogenesis by activating the Raf-1/MEK/ERK- and PI3K/Akt/eNOS-dependent signal pathways. Am. J. Physiol. Heart Circulat. Physiol. 291, H2836–2846.
Lepiller, S., Franche, N., Solary, E., Chluba, J., Laurens, V., 2009. Comparative analysis of zebrafish nos2a and nos2b genes. Gene 445, 58–65.
Lindsey, B.W., Dumbarton, T.C., Moorman, S.J., Smith, F.M., Croll, R.P., 2011. Effects of simulated microgravity on the development of the swimbladder and buoyancy control in larval zebrafish (Danio rerio). J. Experim. Zool. Part A Ecol. Genet. Physiol. 315, 302–313.
Liu, T., Li, X., Sun, X., Ma, X., Cui, Z., 2004. Analysis on forces and movement of cultivated particles in a rotating wall vessel bioreactor. Biochem. Eng. J. 18, 97–104.
Mariotti, M., Maier, J.A.M., 2008. Gravitational unloading induces an anti-angiogenic phenotype in human microvascular endothelial cells. J. Cell. Biochem. 104, 129–135.
Moncada, S., Higgs, E.A., Hodson, H.F., Knowles, R.G., Lopez-Jaramillo, P., McCall, T., Palmer, R.M.J., Radomski, M.W., Rees, D.D., Schulz, R., 1991. The l-Arginine: nitric oxide pathway. J. Cardiovasc. Pharmacol. 17, S1–S9.
Moorman, S.J., Cordova, R., Davies, S.A., 2002. A critical period for functional vestibular development in zebrafish. Devel. Dynam. : Off. Publ. Am. Associat. Anatomists 223, 285–291.
Murohara, T., Asahara, T., Silver, M., Bauters, C., Masuda, H., Kalka, C., Kearney, M., Chen, D., Symes, J.F., Fishman, M.C., Huang, P.L., Isner, J.M., 1998. Nitric oxide synthase modulates angiogenesis in response to tissue ischemia. J. Clin. Investig. 101, 2567–2578.
Namkoong, S., Chung, B.-H., Ha, K.-S., Lee, H., Kwon, Y.-G., Kim, Y.-M., 2008. Microscopic technique for the detection of nitric oxide-dependent angiogenesis in an animal model. Methods Enzymol 441, 393–402.
Namkoong, S., Lee, S.J., Kim, C.K., Kim, Y.M., Chung, H.T., Lee, H., Han, J.A., Ha, K.S., Kwon, Y.G., Kim, Y.M., 2005. Prostaglandin E2 stimulates angiogenesis by activating the nitric oxide/cGMP pathway in human umbilical vein endothelial cells. Exp. Mol. Med. 37, 588–600.
Pelster, B., Grillitsch, S., Schwerte, T., 2005. NO as a mediator during the early development of the cardiovascular system in the zebrafish. Comparat. Biochem. Physiol. Part A Mol. Integr. Physiol. 142, 215–220.
Rudic, R.D., Shesely, E.G., Maeda, N., Smithies, O., Segal, S.S., Sessa, W.C., 1998. Direct evidence for the importance of endothelium-derived nitric oxide in vascular remodeling. J. Clin. Investigat. 101, 731–736.
Sessa, W.C., 2009. Molecular control of blood flow and angiogenesis: role of nitric oxide. J. Thrombosis Haemostasis : JTH 7 (Suppl 1), 35–37.
Shi, F., Wang, Y.C., Zhao, T.Z., Zhang, S., Du, T.Y., Yang, C.B., Li, Y.H., Sun, X.Q., 2012. Effects of simulated microgravity on human umbilical vein endothelial cell angiogenesis and role of the PI3K-Akt-eNOS signal pathway. PloS One 7, e40365.
Siamwala, J.H., Majumder, S., Tamilarasan, K.P., Muley, A., Reddy, S.H., Kolluru, G.K., Sinha, S., Chatterjee, S., 2010. Simulated microgravity promotes nitric oxide-supported angiogenesis via the iNOS-cGMP-PKG pathway in macrovascular endothelial cells. FEBS Lett. 584, 3415–3423.
Sun, T., Xie, X., Zhang, J.Q., Bao, J., Tang, C.Z., Lei, D.X., Qiu, J.H., Wang, G.X., 2013. [Effect of horizontal rotary culture on zebrafish vascular development]. Yi chuan = Hereditas 35, 502–510.
Uruno, A., Sugawara, A., Kanatsuka, H., Arima, S., Taniyama, Y., Kudo, M., Takeuchi, K., Ito, S., 2004. Hepatocyte growth factor stimulates nitric oxide production through endothelial nitric oxide synthase activation by the phosphoinositide 3-kinase/Akt pathway and possibly by mitogen-activated protein kinase kinase in vascular endothelial cells. Hyperten. Res.: Off. J. Jpn. Soc. Hyperten. 27, 887–895.
Xie, X., Zhou, T., Wang, Y., Chen, H., Lei, D., Huang, L., Jin, X., Sun, T., Tan, J., Yin, T., 2018. Blood flow regulates Zebrafish caudal Vein Plexus angiogenesis by ERK5-klf2a-nos2b signaling. Curr. Mol. Med. 18, 3–14.
Yancopoulos, G.D., Davis, S., Gale, N.W., Rudge, J.S., Wiegand, S.J., Holash, J., 2000. Vascular-specific growth factors and blood vessel formation. Nature 407, 242–248.
Ziche, M., Morbidelli, L., Choudhuri, R., Zhang, H.T., Donnini, S., Granger, H.J., Bicknell, R., 1997. Nitric oxide synthase lies downstream from vascular endothelial growth factor-induced but not basic fibroblast growth factor-induced angiogenesis. J. Clin. Investig. 99, 2625–2634.